Y. M. Hill
N. O. Reckord
D. R. Winner

A General Method for Obtaining Impedance and Coupling Characteristics of Practical Microstrip and Triplate Transmission Line Configurations

Abstract: In order to design an interconnection system for nanosecond-risetime logic circuitry, it is necessary to obtain a balance between impedance variations, propagation velocities, and crosstalk levels so as to achieve the best system speed as well as system speed control. To accomplish this, it is necessary to relate the electrical material properties and physical dimensions of the connections to characteristic impedances, propagation velocities, and crosstalk coupling coefficients.

Two practical transmission line configurations: the microstrip line, which is coated for physical protection, and the offset or unsymmetrical triplate line, are being fabricated by mass production techniques. Because of the close control required and the many factors affecting impedance and coupling, these configurations require accurate means for predicting their characteristics.

An improved "subintervals" technique and a series approximating the Green's function have been combined to yield a single practical computer algorithm. Excellent agreement has been obtained in comparing the results of computations with large scale-model transmission line measurements. The method is quite general because dimensions, conductor shapes, and dielectric properties may vary widely.

Introduction

The close control of the overall performance of the logic circuits in a high performance computer is a function of the variations of internal circuit parameters, connection characteristics, operating temperatures, and power supply voltages. The variation in connection characteristics is a matter of load-point distribution and system interconnection design. In particular, this paper relates to the latter problem, that of designing interconnecting transmission lines. The characteristics that must be predicted and controlled are the (1) characteristic impedances, (2) propagation velocities, and (3) crosstalk coupling coefficients.

Two transmission line configurations are the microstrip line and the triplate line outlined in Figs. 1a and 1b, respectively. As shown in Fig. 1a, the microstrip line is embedded in a dielectric slab. This condition is a result of a post-etch coating which is intended for physical protection of the line. The lines are shown with trapezoidal cross sections, a characteristic of etched lines. This figure also indicates that coupling between lines of different widths is required. Figure 1b shows that the triplate configuration may be highly unsymmetrical.

For preliminary design, curves are required that give impedance, propagation velocity, and crosstalk parameters to an accuracy of a few percent. For product control, it must be possible to predict the impedance and propagation velocity characteristics of the actual line configuration to an accuracy of within 1% of their true values. This paper describes the multiple-image/subintervals (MISI) technique that, when programmed for a computer like the IBM System/360 Model 65, enables the user to obtain this information.

The relation of this paper to the large amount of existing literature on the subject will be detailed by referring to instances in which aspects of our solution have been handled. First, the solution presented in this paper makes use of a Green's function in infinite series form that is analogous to Maxwell's solution for the field of a point source in the presence of, but outside, two parallel material boundaries.[1] Second, our solution employs an improved finite subinterval technique related to that employed by Black and Higgins,[2] and we extend this technique to cover the crosstalk coefficients. Cristal[3] computes crosstalk parameters for special triplate cases and approximates Neumann boundary conditions. The technique in our paper avoids approximate boundary conditions and uses completely defined Dirichlet boundary conditions. Wheeler[4] has presented solutions for the impedance of rectangular lines in and on dielectric slabs using con-

Hill and Reckord are with the Components Division and Winner is with Systems Development Division, all in Endicott, New York.

formal transformations. Cohn[5,6] has provided solutions for the odd- and even-mode impedances of symmetric coupled triplate lines. Guckel[7] has bounded the impedances of single, rectangular, triplate lines with good accuracy. Finally, Arvanitakis, Kolias, and Radzelovage[8] indicate how the crosstalk coupling coefficients can be used in a rather general way to predict crosstalk waveforms.

The MISI technique is proposed in this paper as a single method providing impedance, velocity, and coupling coefficients for the cases covered in the papers mentioned, and for arbitrary line cross sections and line locations as well.

The transmission line approximation

We propose to derive characteristic impedances, propagation velocities, and coupling coefficients by providing a two-dimensional solution of LaPlace's equation for the electric field. The following arguments show that this is applicable.

For computer interconnections it seems reasonable to assume a TEM mode in spite of the dielectric slab inhomogeneity. The very high speed, closely timed logic nets tend to be in the order of one foot in length. This distance is long with respect to wave travel during the switching transition time, τ_r, but short enough so that appreciable distortion of the pulse edge due to separate air and dielectric propagation velocities does not take place. As computer speeds increase, it is reasonable to expect that circuit densities will increase and line lengths will decrease. Thus, dispersion effects should remain approximately constant.

There is also the question of whether the conductor skin impedance is so appreciable as to affect measurements. An exact resolution of this question is beyond the scope of this paper. However, using simple round-wire relationships,[9] one can estimate appreciable skin impedance to occur when the internal line inductance, L_i, approaches a small fraction of the external line inductance, L_e. Here

$$L_i = \frac{1}{\pi d}\sqrt{\frac{\mu}{4\pi\sigma f}} = \frac{1}{\pi d}\sqrt{\frac{\mu}{4\pi\sigma}\frac{\tau_r}{0.42}}$$

and

$$L_e = \frac{Z_0\sqrt{\epsilon_r'}}{v_0},$$

where d is the wire diameter, μ the permeability, σ the conductivity, ϵ_r' the apparent relative permittivity, v_0 the velocity in vacuum, and f the frequency. Assuming the use of copper lines and $L_i = 0.015\ L_e$, it is possible to derive the useful expression,

$$d > \frac{400}{Z_0}\sqrt{\frac{\tau_r}{\epsilon_r'}} \qquad \text{(MKS units)}.$$

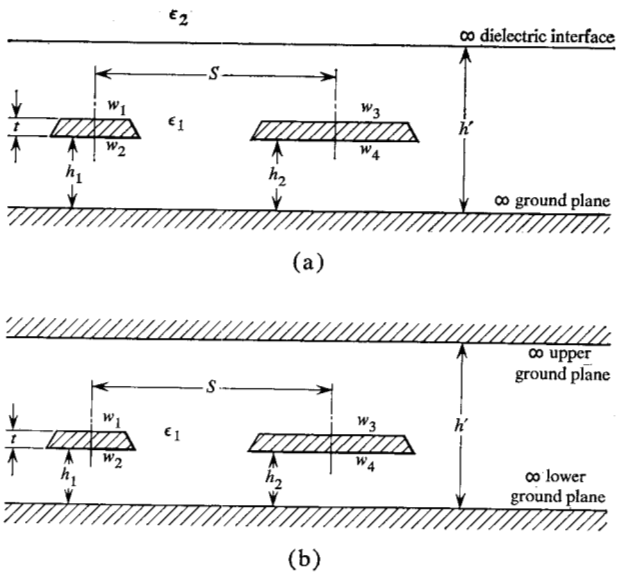

Figure 1 Transverse cross sections of typical lines; (a) microstrip lines, (b) triplate lines.

Thus, for $\tau_r = 200$ picoseconds, $\epsilon_r' = 4$ and $Z_0 = 50\Omega$, $d > 57\ \mu$m($\sim$2.3 mils). This suggests that for these conditions, the impedance results of this paper should be refined for skin effects when a conductor dimension is in this range or smaller.

If Maxwell's equations hold and, in particular, if $\mathbf{E}$, $\mathbf{B}$, μ, $\mathbf{A}$, and ϕ represent the electric field, the magnetic field, the permeability, the vector potential and the scalar potential respectively, then

$$\nabla \times \mathbf{E} + \frac{\partial \mathbf{B}}{\partial t} = 0.$$

Also, if

$$\mathbf{B} = \nabla \times \mathbf{A},$$

then

$$\nabla \times \left(\mathbf{E} + \frac{\partial \mathbf{A}}{\partial t}\right) = 0.$$

Since $\nabla \times (-\nabla\phi) \equiv 0$, where ϕ is some scalar point function, then

$$\mathbf{E} = -\nabla\phi - \frac{\partial \mathbf{A}}{\partial t}.$$

In terms of the charge and current density, we then have for the field at time t and at $\mathbf{r}$:

$$\mathbf{E} = -\nabla\left(\frac{1}{4\pi\epsilon}\int \frac{\rho'\,dv'}{|\mathbf{r} - \mathbf{r}'|}\right) - \frac{\partial}{\partial t}\left(\frac{\mu}{4\pi}\int \frac{\mathbf{J}'\,dv'}{|\mathbf{r} - \mathbf{r}'|}\right),$$

where ρ' and $\mathbf{J}'$ are the charge and current densities in the volume element dv' at time $[t - (|\mathbf{r} - \mathbf{r}'|/v)]$. Also, v is the propagation velocity in the medium with permittivity ϵ and permeability μ.

The exact calculation of the electric field involves a knowledge of the retarded source distributions. In our problem, the retarded effects appear negligible since the sources of interest are only a few thousandths of an inch away from each other, and since the pulse transition distance, $l_r = v\tau_r$, is several inches long. Also, estimating magnitudes of the two terms in the expression for **E** leads to the conclusion that the contribution of the second term may be safely neglected. Therefore, the electric field at any position along the line may be calculated from

$$\mathbf{E} = -\nabla\phi,$$

and since the longitudinal component is negligible, it is possible to use a two-dimensional solution of LaPlace's equation when the transmission line cross section is constant.

Knowing the electric field at any point, we can compute the total charge on a conductor by integrating the normal component of the electric displacement over the conductor. Also, we can integrate the electric field from one conductor to the other to find the potential difference between conductors. Then in general, we can calculate the capacitance per unit length of line as

$$C = \frac{\int_S (\mathbf{D}\cdot\hat{\mathbf{n}})\, ds}{\int_P \mathbf{E}\cdot d\mathbf{l}},$$

where $\hat{\mathbf{n}}$ is a unit vector normal to the conductor surface element ds, S is a unit length of conductor surface, and $d\mathbf{l}$ is a directed element of path P, which joins the two conductors.

If we neglect losses, current penetration and internal inductance effects, we can make use of the following relations for a single, isolated line:

$$Z_0 = \sqrt{\frac{L_i}{C_i}} = \frac{1}{vC_i} = \frac{1}{v_0\sqrt{C_iC_{i0}}},$$

$$v = v_0\sqrt{\frac{C_{i0}}{C_i}},$$

where

Z_0 = characteristic impedance of the line,
L_i = self-inductance per unit length of line i,
v = propagation velocity in the medium,
v_0 = propagation velocity in vacuum. (The subscript 0, when used with velocities, capacitances and coupling coefficients, is used to denote the absence of dielectrics, i.e., vacuum.)
C_i = self-capacitance per unit length of line i. (No other line present.)
C_{i0} = self-capacitance per unit length of line i in a vacuum.

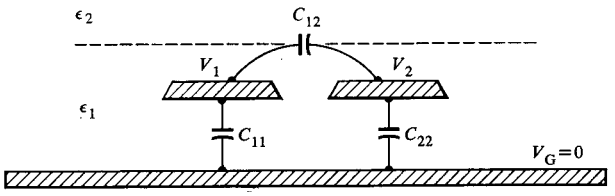

Potential assignments		Results obtainable
V_1	V_2	
1	1	$\sum_1 w_i\sigma_i = C_{11}$
		$\sum_2 w_i\sigma_i = C_{22}$
1	0	$\sum_1 w_i\sigma_i = C_{11}+C_{12}$
		$\left\lvert\sum_2 w_i\sigma_i\right\rvert = C_{12}$
0	1	$\left\lvert\sum_1 w_i\sigma_i\right\rvert = C_{12}$
		$\sum_2 w_i\sigma_i = C_{22}+C_{12}$
1	Unknown	$\sum_1 w_i\sigma_i = C_{11}+\frac{C_{12}C_{22}}{C_{12}+C_{22}}$
		$V_2 = K_{12}$
Unknown	1	$\sum_2 w_i\sigma_i = C_{22}+\frac{C_{12}C_{11}}{C_{11}+C_{12}}$
		$V_1 = K_{21}$

Figure 2 Interpretation of MISI results for two-conductor case.

For coupled parallel lines, coupling coefficients are defined as follows:

$$K_{Lij} = \frac{M_{ij}}{\sqrt{L_iL_j}},$$

$$K_{Cij} = \frac{C_{ij}}{C_{ij} + C_{ii}},$$

$$K_{Cij0} = \frac{C_{ij0}}{C_{ij0} + C_{ii0}},$$

where

M_{ij} = mutual inductance per unit length of line i with respect to line j,
C_{ij} = mutual capacitance per unit length between line i and line j in the presence of specified dielectric materials,
C_{ii} = direct capacitance per unit length of line i to ground in the presence of specified dielectric materials and other signal conductors charged to the potential of line i.

We will assume $K_{Lij} = K_{Cij0}$ in view of the negligible current penetration during the time of crosstalk production.

In dealing with multiconductor systems, one must be aware that several "capacitances" can be calculated or measured depending on the charge/voltage assignments of the conductors. For instance, in a two-line over ground plane system, C_1', the capacitance per unit length of line 1 with the other line floating and uncharged, can be calculated or measured as

$$C_1' = C_{11} + \frac{C_{12}C_{22}}{C_{12} + C_{22}} = C_{11}(1 + K_{C_{12}})$$

when $C_{11} = C_{22}$.

Of course, $C_1' \longrightarrow C_1$ as $K_{C12} \longrightarrow 0$ since we are now returning to the single isolated line case. Other potential assignments and resultant capacitances will be discussed in the following paragraphs.

It is the task of the MISI technique to provide a means for computing the various capacitances C_i, C_{ij}, C_{i0}, C_{ij0} and the coupling coefficients K_{Cij0} and K_{Cij}. The appropriate capacitances are determined in the following manner:

a. The perimeter of each conductor cross section is divided into subintervals, each having an unknown constant charge density.

b. The required charge distribution is that distribution which, in the presence of the prescribed ground plane(s) and dielectric interface, produces the specified conductor potentials.

c. The capacitances (per unit length) are calculated as the ratios of conductor charge (per unit length) to conductor potential.

d. The appropriate coupling coefficient is found as the ratio of the voltage induced on an inactive conductor to the voltage specified on an active conductor. Figure 2 outlines possible potential assignments and specifies the computation necessary for each C_{ij} and K_{ij}. In the figure, w_i = width of the i-th subinterval, σ_i = surface charge density on the i-th subinterval, and $\sum_N$ indicates a summation of charge on the subintervals of conductor N.

The subintervals technique

A formal description of the subintervals technique is now presented. The two-dimensional solution to LaPlace's equation, namely,

$$V(\mathbf{r}) = -\frac{1}{2\pi\epsilon}\int \sigma(\mathbf{r}') \ln |\mathbf{r} - \mathbf{r}'| \, ds', \qquad (1)$$

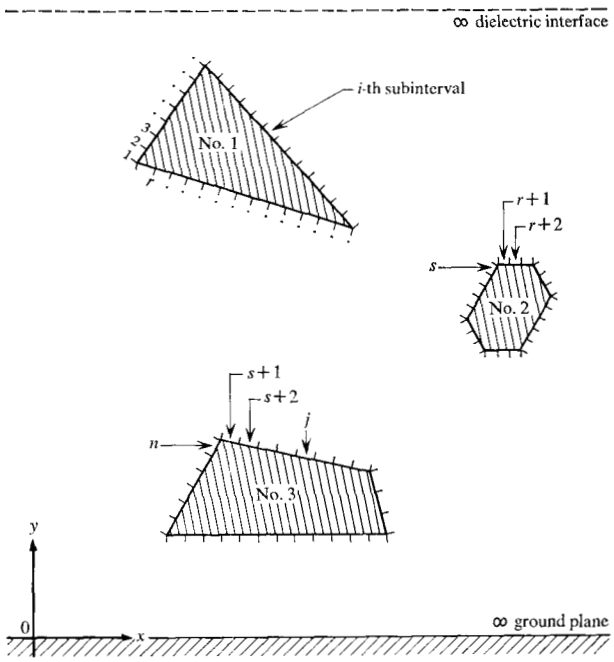

Figure 3 Subdivision of conductor boundaries.

may be viewed as an integral equation in $\sigma(\mathbf{r})$ for which we can specify the boundary conditions explicitly on the active conductors and implicitly on the inactive conductors. Each inactive conductor, Q_l, adds an unknown potential, V_l, and an additional integral equation

$$0 = \int_{Q_l} \sigma(\mathbf{r}) \, ds, \quad \text{where} \quad l = 1, 2, \cdots, q. \qquad (2)$$

We can subdivide the perimeters of the conductors into n subintervals as in Fig. 3, each of width w_i and each having an unknown but constant surface charge density σ_i. For the moment disregard the infinite ground plane and dielectric interface in Fig. 3. The subdivision allows Eqs. (1) and (2) to be approximated by discrete sums as follows:

$$V_i = \sum_{j=1}^{n} p_{ij}\sigma_j, \qquad i = 1, 2, \cdots, n, \qquad (3)$$

where

$$p_{ij} = -\frac{1}{2\pi\epsilon}\int_{w_j} \ln |\mathbf{r}_i - \mathbf{r}_j| \, ds_j; \qquad (4)$$

and

$$0 = \sum_{Q_l} w_i\sigma_j, \qquad l = 1, 2, \cdots, q, \qquad (5)$$

where the sum $\sum_{Q_l}$ is taken over the subintervals of each inactive conductor l. V_i is calculated at the midpoint of the i-th subinterval.

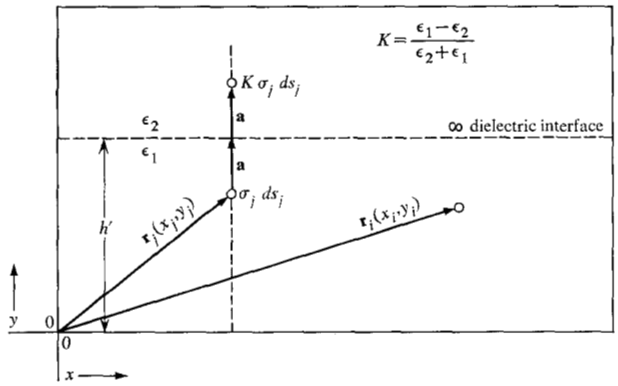

Figure 4 Infinite dielectric interface.

For physical reasons in the transversely finite conductor case being considered, it is necessary that

$$\sum_{j=1}^{n} w_j\sigma_j = 0, \tag{6}$$

where the summation extends over all conductors.

But with Eqs. (3), (5), and (6), there are $n + q + 1$ equations in $n + q$ unknowns. Making use of the fact that a constant also satisfies LaPlace's equation, we can form

$$V_i - V_1 = \sum_{j=1}^{n} (p_{ij} - p_{1j})\sigma_j, \qquad i = 2, 3, \cdots n, \tag{7}$$

where the summation extends over all conductors, and $n + q$ equations result. Thus, the transversely finite conductor case can be solved.

In order to treat problems involving one or more infinite ground planes, we will not make explicit use of Eqs. (6) and (7). For instance, let the infinite ground plane, but not the dielectric interface, exist in Fig. 3; and let it be required to solve the resultant problem. By substituting for Eq. (4),

$$p_{ij} = -\frac{1}{2\pi\epsilon}\int_{w_j} [\ln|\mathbf{r}_i - \mathbf{r}_j| - \ln|\mathbf{r}_i - \mathbf{r}'_j|]\,ds_j,$$

where $\mathbf{r}'_j$ is the image of position $\mathbf{r}_j$ with respect to the ground plane, we can solve for the charge densities σ_j required to satisfy the potential values on the conductors as well as the boundary conditions along the infinite ground plane. By the use of images, Eq. (6) is implicitly satisfied. Also, this procedure means that subintervals are needed only for the conducting surfaces that are apart from the ground plane.

It has been suggested[2] that for p_{ij} where $i \neq j$, Eq. (4) be replaced by

$$p_{ij} = -\frac{1}{2\pi\epsilon}\ln|\mathbf{r}_i - \mathbf{r}_j|\cdot w_j.$$

This can lead to serious errors for subintervals of different lengths and arbitrary placement. Considerable advantage is gained by the numerical evaluation of the integral in Eq. (4).

Next, we consider the problem of meeting the boundary conditions along the ground plane and a second parallel boundary which may either be a dielectric interface or second ground plane.

A series for the Green's function of a dielectric interface parallel to an infinite ground plane

The problem is to replace the function

$$dV_i = -\frac{\sigma_j\,ds_j}{2\pi\epsilon}(\ln|\mathbf{r}_i - \mathbf{r}_j| - \ln|\mathbf{r}_i - \mathbf{r}'_j|)$$

with a potential function that simultaneously satisfies the boundary conditions on the dielectric interface and on the ground plane. Such a function will be used to compute the p_{ij} in the presence of the interface and ground plane.

The boundary conditions at each point on a dielectric interface between regions having ϵ_1 and ϵ_2 permittivities are

$$\epsilon_1\left.\frac{\partial V}{\partial \mathbf{n}}\right|_{R_1} = \epsilon_2\left.\frac{\partial V}{\partial \mathbf{n}}\right|_{R_2},$$

and

$$\left.\frac{\partial V}{\partial \mathbf{s}}\right|_{R_1} = \left.\frac{\partial V}{\partial \mathbf{s}}\right|_{R_2},$$

where $\mathbf{n}$ is a position vector taken in the direction normal to the dielectric interface, $\mathbf{s}$ is a position vector taken parallel to the interface, and R_1 and R_2 are points arbitrarily close to the interface in the ϵ_1 and ϵ_2 regions respectively. This assumes no surface charge.

The boundary conditions at each point on an interface between a dielectric and a conductor are

$$\epsilon_2\left.\frac{\partial V}{\partial \mathbf{n}}\right|_{R_2'} = \sigma,$$

and

$$\left.\frac{\partial V}{\partial \mathbf{s}}\right|_{R_2'} = 0,$$

where $\mathbf{n}$ is in the outward normal direction from the conductor surface, and $\mathbf{s}$ is parallel to the surface; R'_2 is arbitrarily close to the surface but in the ϵ_2 region. σ is the surface charge density on the conductor.

We shall now consider a simple dielectric interface. It is easy to show, following the method outlined[10] for point charges, that, for the arrangement shown in Fig. 4, the potential in the ϵ_1 region is given by

$$dV_i = -\frac{\sigma_j\,ds_j}{2\pi\epsilon_1}[\ln|\mathbf{r}_i - \mathbf{r}_j| + K\ln|\mathbf{r}_i - \mathbf{r}_j - 2\mathbf{a}|], \tag{8}$$

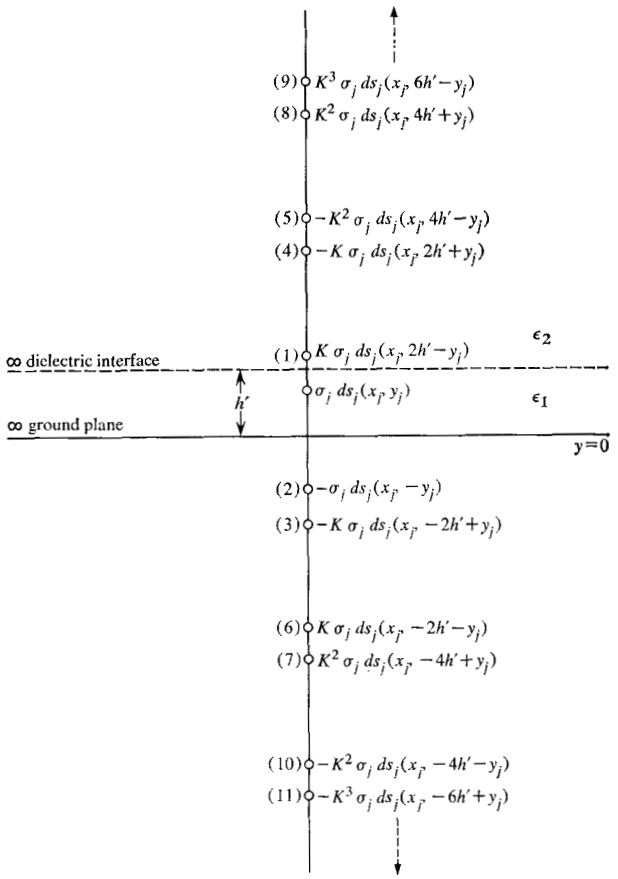

Figure 5 Construction of an infinite series of image charges for two parallel infinite plane boundaries.

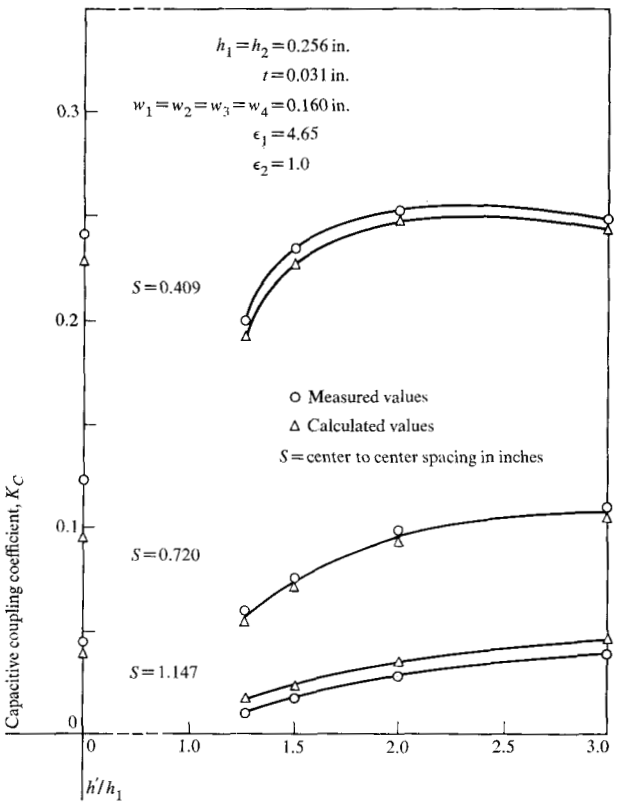

Figure 6 Calculated and measured capacitive coupling coefficient, K_C vs. height of dielectric interface above ground divided by height of line above ground, h'/h_1.

where

$$K = \frac{\epsilon_1 - \epsilon_2}{\epsilon_1 + \epsilon_2}$$

and **a** is the vector from ds_i to the interface.

Many useful capacitance problems can be solved by using the preceding equations to form the basis of a computer algorithm. As suggested in Fig. 2, capacitances and coupling coefficients can be calculated by assigning appropriate potentials and solving for the σ_i (and V_i).

In order to satisfy the boundary conditions on a parallel ground plane as well as the dielectric interface, an infinite set of image charges is derived for each charge element $\sigma_j\, ds_j$. With reference to Fig. 5, first, reflect the original line charge $\sigma_j\, ds_j$ at (x_j, y_j) about the dielectric interface, second, reflect about the ground plane, third reflect about the interface, etc. to obtain a sequence of line image charges as follows:

Reflection	*Resultant line image charge*
About the interface:	$K\sigma_j\, ds_j$ at $(x_j, 2h' - y_j)$
About the ground plane:	$-\sigma_j\, ds_j$ at $(x_j, -y_j)$ and $-K\sigma_j\, ds_j$ at $(x_j, -2h' + y_j)$
About the interface:	$-K\sigma_j\, ds_j$ at $(x_j, 2h' + y_j)$ and $-K^2\, \sigma_j\, ds_j$ at $(x_j, 4h' - y_j)$
About the ground plane:	$K\sigma_j\, ds_j$ at $(x_j, -2h' - y_j)$ and $K^2\sigma_j\, ds_j$ at $(x_j, -4h' + y_j)$.

Continuing the above procedure, the final result will be an infinite sequence of line image charges. The potential of such a sequence of line charges (including the original) within the region bounded by the ground plane and the dielectric interface is as follows:

$$\begin{aligned} dV_i = -\frac{\sigma_j\, ds_j}{4\pi\epsilon_1} \Big\{ & \ln\left[(x_i - x_j)^2 + (y_i - y_j)^2\right] \\ & - \ln\left[(x_i - x_j)^2 + (y_i + y_j)^2\right] \\ & + \sum_{n=1}^{\infty} (-1)^n K^n \\ & \times \{\ln\left[(x_i - x_j)^2 + (y_i - 2nh' - y_j)^2\right] \\ & - \ln\left[(x_i - x_j)^2 + (y_i - 2nh' + y_j)^2\right] \\ & + \ln\left[(x_i - x_j)^2 + (y_i + 2nh' - y_j)^2\right] \\ & - \ln\left[(x_i - x_j)^2 + (y_i + 2nh' + y_j)^2\right]\} \Big\}. \end{aligned}$$

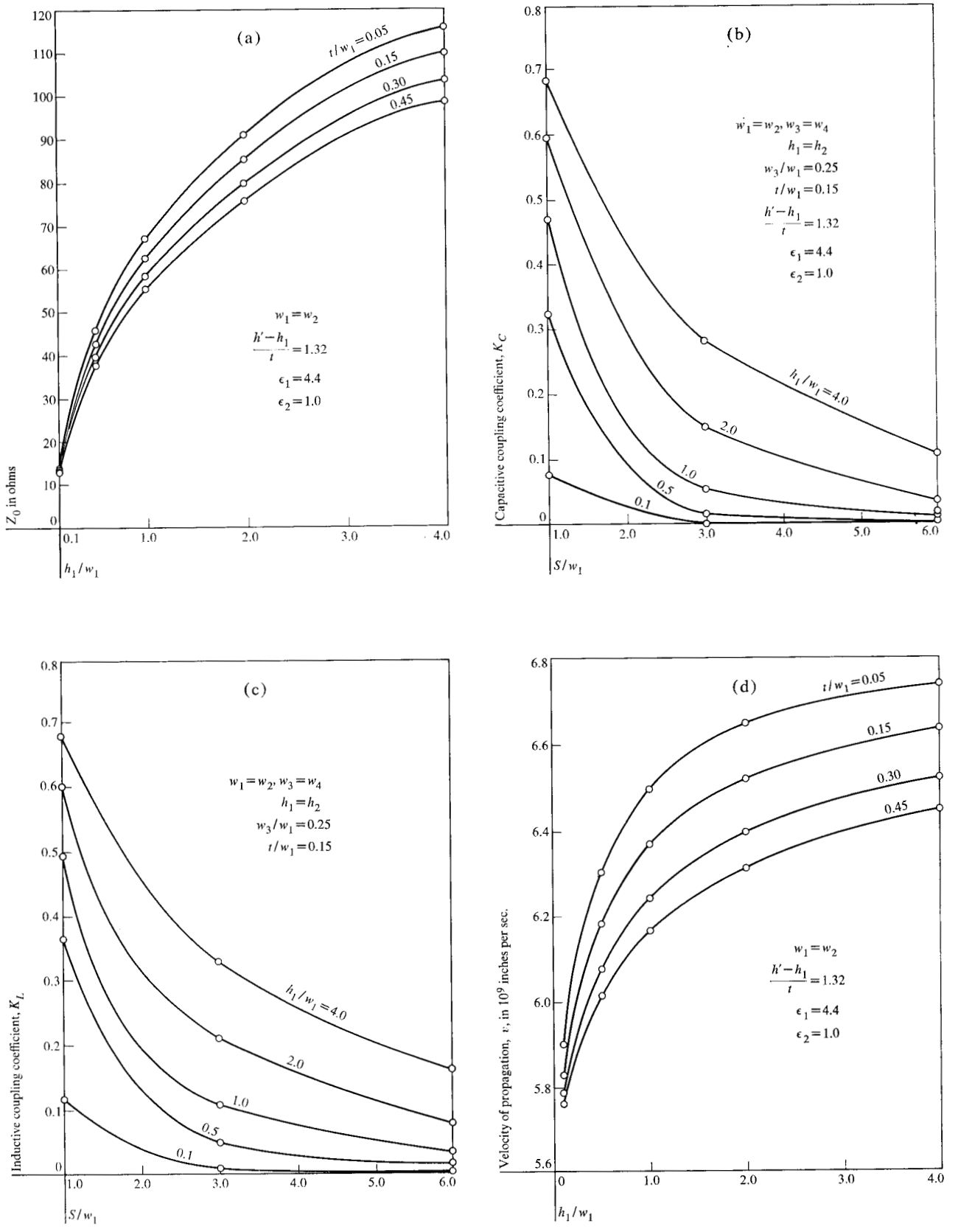

Figure 7 Design curves for microstrip lines; (a) characteristic impedance, (b) capacitive coupling coefficient, (c) inductive coupling coefficient, (d) velocity of propagation.

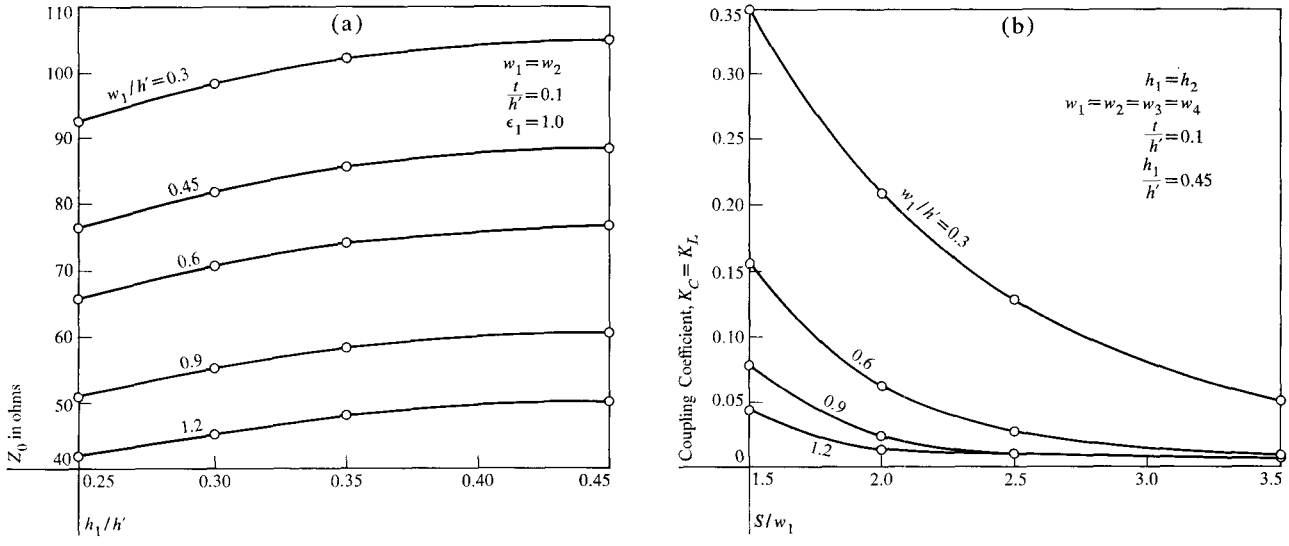

Figure 8 Design curves for triplate lines; (a) characteristic impedance, (b) coupling coefficient.

Table 1 Comparison of experimental and calculated values for C_{10}

w in in.	t in in.	h in in.	h' in in.	$C_{10(Calc)}$ in pF	$C_{10(Meas)}$ in pF	$\frac{C_{Meas}-C_{Calc}}{C_{Calc}}\times 100$ in percent
0.400	0.080	0.230	0.611	1.240	1.265	+2.0
0.400	0.080	0.450	1.343	0.784	0.791	+0.9
0.400	0.080	0.830	1.800	0.649	0.656	+1.1

This expression can be shown to satisfy the appropriate boundary conditions along the ground plane, as well as along the dielectric interface. The simplest argument is to note that, in Fig. 5, equal and opposite charges are equidistant above and below the ground plane, while for the interface, the equidistant charges are always in the ratio 1 : K. Thus, assuming linearity and invoking superposition, we have satisfied the boundary conditions. It is also possible to construct a potential function valid in the region of ϵ_2 and by differentiation prove that the boundary conditions are met. We will compare predictions with measurements in order to further validate results.

Comparison with measurements for microstrip K_C

Attempting to prove the adequacy of a computational technique by using actual etched lines presents many difficulties attendant with measuring and/or controlling very small line cross sections and conductor spacings, and with determining the electrical characteristics of very thin epoxy glass laminates and coatings. For this reason, it has proven instructive to build large, scale-model line configurations and then to make bridge capacitance measurements at 1 MHz. Models were constructed with appropriately guarded end sections. The dielectric constant of the liquid was measured in a precision sample holder at the frequency of the scale-model measurement. Corrections were estimated for mechanical set up errors. Figure 6 shows how calculated and measured values of $K_{Cij} = C_{ij}/(C_{ij} + C_{ij})$ compare for various dielectric heights, h'.

Triplate theory and comparison with measurements

Note that the dielectric interface may be replaced by a second ground plane by setting $K=(\epsilon_1-\epsilon_2)/(\epsilon_1+\epsilon_2)=-1$. This results in the triplate solution. In order to verify the triplate results, another large scale model is currently being used. The dielectric is air. The results for C_{10}, available at this time, are shown in Table 1.

Computation results

The MISI technique has been used to produce graphs for Z_0, K_C, K_L, and v. Figures 7a–d give results for certain

microstrip configurations and Figs. 8a and b are results for triplate configurations. The impedance and velocity information for the triplate configurations in the presence of an arbitrary dielectric can be obtained from the following equations:

$$Z_0 = Z_{00}/\sqrt{\epsilon_r},$$

$$v = v_0/\sqrt{\epsilon_r},$$

where Z_{00} is the characteristic impedance in vacuum.

The curves of Figs. 7a and 7d, when compared to the existing results for uncoated lines, predict that impedances and velocities of coated 40 to 60-ohm configurations will be decreased by about 8 to 10% for $t/w = 0.25$, $(h' - h_1)/t = 1.32$, and $\epsilon_r = 4.4$.

The triplate curves of Fig. 8 are new results in that asymmetrical cases, $h_1 \neq (h' - t)/2$, are covered for Z_0, and coupling for the worst case, $h_1 = (h' - t)/2$, is covered.

A great number of curves might be generated. The effort has been to cover some of the more interesting and useful cases.

Earlier we mentioned that trapezoidal line cross sections might be accommodated. The effect has been investigated in a 50-ohm triplate design where $t/w = 0.15$ and $h_1/h' = 0.3$. The base angle was varied between 60° and 90°, and the average change in Z_0 was $\pm 2.1\%$ for a $\mp 15°$ change in angle.

Conclusions

A new computational technique for uniform transmission lines has been presented. This technique gives results that agree very well with experimental data for capacitance and coupling coefficients in cases that, to the authors' knowledge, have not been presented before. The method has a wide range of application because one can obtain highly accurate results for characteristic impedance, propagation velocity, and crosstalk coupling coefficients for practical microstrip and triplate line configurations.

References

1. J. C. Maxwell, *A Treatise on Electricity and Magnetism,* Dover Publications, Inc., New York, 1954, p. 443.
2. K. G. Black and T. J. Higgins, "Rigorous Determination of the Parameters of Microstrip Transmission Lines," *Transactions IRE* **MTT-3,** 93–113 (1955).
3. E. G. Cristal, "Coupled Circular Cylindrical Rods Between Parallel Ground Planes," *Transactions IEEE* **MTT-12,** 428–439 (1964).
4. H. A. Wheeler, "Transmission-Line Properties of Parallel Strips Separated by a Dielectric Sheet," *Transactions IEEE* **MTT-14,** 172–185 (1966).
5. S. B. Cohn, "Characteristic Impedance of the Shielded-Strip Transmission Line, *Transactions IRE* **MTT-2,** 52–57 (1954).
6. S. B. Cohn, "Shielded Coupled-Strip Transmission Line," *Transactions IRE* **MTT-3,** 29–38 (1955).
7. H. Guckel, "Characteristic Impedances of Generalized Rectangular Transmission Lines," *Transactions IEEE* **MTT-13,** 270–274 (1965).
8. N. C. Arvanitakis, J. T. Kolias, and W. Radzelovage, "Coupled Noise Prediction in Printed Circuit Boards for a High Speed Computer System," *Symposium Record, 7th International Electronic Circuit Packaging Symposium,* 1966.
9. S. Ramo and J. R. Whinnery, *Fields and Waves in Modern Radio,* John Wiley and Sons, New York, 1944, p. 209 ff.
10. J. D. Jackson, *Classical Electrodynamics,* John Wiley and Sons, New York, 1962, p. 110 ff.

Received September 5, 1969